Computers & Structures Vol. 33, No. 5, pp. 1191–1204, 1989
Printed in Great Britain.

0045-7949/89 $3.00 + 0.00

HIGHER-ORDER THEORIES FOR COMPOSITE AND SANDWICH CYLINDRICAL SHELLS WITH C^0 FINITE ELEMENT

T. KANT† and M. P. MENON
Department of Civil Engineering, Indian Institute of Technology, Powai, Bombay 400 076, India

(*Received* 3 *November* 1988)

Abstract—A higher-order displacement model for the behaviour of symmetric and unsymmetric laminated composite and sandwich cylindrical shells based on C^0 finite element discretization is presented. Two theories, namely, (1) Geometrically Thin Shell Theory, based on the assumption that the ratio of the shell thickness to radius (h/R) is less than unity, and (2) Geometrically Thick Shell Theory, in which $(h/R)^2 \ll 1$, are developed. These theories incorporate a more realistic non-linear variation of longitudinal displacements through the shell thickness and thus eliminate the use of shear correction coefficients. The influence of (h/R) for a thick shell is studied and the results are compared with those of geometrically thin shell theory and other available results.

INTRODUCTION

A shell of revolution is an important structural component in all industrial applications, especially those relating to nuclear, aerospace and petrochemical engineering. The multilayered composites are important structural materials in weight sensitive aerospace applications, where high strength-to-weight and stiffness-to-weight ratios are desired. Such composites, idealized as orthotropic lamina, are bonded together to form a laminate and are used as structural components.

The finite element formulation provides a convenient method of solution for such laminated composites having complex geometry, arbitrary loadings and boundary conditions.

Any two-dimensional shell theory is an approximation of real three-dimensional elasticity problems. The solution of problems in three-dimensional theory of elasticity involves vast complications, which are overcome only in a few special cases.

In a shell theory the three-dimensional system is reduced to a two-dimensional one by deploying a set of simplifying assumptions. The classical Love's thin shell theory is based on Kirchhoff's hypothesis. It assumes the laminae to be in the state of plane stress and neglects the effects of transverse shears and normal strain in the thickness direction. The first thin shell theory for laminated orthotropic material was developed by Ambartsumyan [1]. This author assumed that the individual orthotropic layers were oriented such that the principal axes of material symmetry coincided with that of the principal coordinates of the shell reference surface. This theory also incorporates the bending–stretching coupling due to unsymmetric lamination in composites. Dong and Taylor [2] presented an extension of Donnell's shallow shell theory to thin laminated shells. These theories are based on the Kirchhoff–Love hypothesis in which transverse shear deformation is neglected.

In the case of composite shells, which are generally identified in practice as (i) 'Fibre Reinforced Shells', in which layers of composite material with high ratio of Young's to shear modulli are bonded together, and (ii) 'Sandwich Shells', in which layers of isotropic material with some layers having significantly lower elastic moduli than others are bonded together, the effects of transverse shear deformation are significant and thus Love's theory is inadequate.

In recent years, an attempt has been made to do away with one or more of the foregoing Kirchhoff assumptions. This is to establish a more rigorous base for the numerical analysis of a wide spectrum of shell problems. Dong and Tso [3] were perhaps the first to present a first-order shear-deformation theory, which included the effect of transverse shear deformation through the shell thickness, and then to construct a laminated orthotropic shell theory. The theory is only applicable, however, to cylindrical shells in which the orthotropic axes of each layer coincide with the reference axes of the shell surface. This theory can be regarded as an extension of Love's first-approximation theory for homogeneous isotropic shells. Another refined theory for laminated anisotropic cylindrical shells was presented by Whitney and Sun [4], who derived a set of governing equations and boundary conditions which included both transverse shear deformation and transverse normal strain. Widera and Chung [5] derived a first-approximation theory for the unsymmetric deformation of a non-homogeneous anisotropic cylindrical

† To whom all correspondence should be addressed.

shell through asymptotic integration of elasticity equations.

The second-order transverse shear deformation effects have been included by Kant [6], who has developed governing equilibrium equations for a thick shell theory. The theory is based on a three-term Taylor series expansion of the displacement vector and generalized Hooke's law, which is applicable to orthotropic material having planes of symmetry coincident with the orthogonal reference flame and also for a system comprising layers of different materials. Bhimaraddi [7] has presented a higher-order theory for a cylindrical shell, using assumed displacement form which results in parabolic variation for transverse shear strains and also satisfies shear-free surface boundary conditions, by introducing a function $\zeta(z)$ in the displacement expression, whose first derivative vanishes at the extreme fibres. In another paper, Bhimaraddi and Stevens [8] have given a procedure for developing the governing equilibrium equations for a cylindrical shell using a vectorial approach in a correct and consistent manner. In this paper a few other alternative forms for ζ-function have been given. Rogers and Knight [9] have formulated a linear higher-order finite element which uses a single high displacement order finite element to model through thickness of an axisymmetric composite structure. The displacement order for the inplane directions remains linear while through thickness, a higher order is used. This is achieved by increasing the number of nodes along the thickness direction. Numerical integration for stiffness is evaluated with respect to the varying material property and laminate thickness in each individual element. Murthy and Reddy [10] have proposed a higher-order theory for the analysis of composite cylindrical shells, by expanding the displacement variables in the form of power series and retaining a finite number of terms. The formulation allows for arbitrary variation of inplane displacement. However, all the above works are based on C^1 continuity.

In first-order shear deformation theory we assume a constant shear rotation through the shell thickness and this requires the use of a shear correction coefficient whose accurate prediction for an anisotropic laminated shell is cumbersome and problem dependent. In addition, this theory does not include the effect of cross-sectional warping which is very essential in the case of thick sandwich shells, which are generally composed of a middle weak core sandwiched between stiff facings, and hence a refined theory, which considers more realistic parabolic variations of transverse shear stresses through the thickness and warping of the transverse cross-section, is found essential. Thus a C^0 finite element formulation based on a higher-order displacement model and including the effect of transverse shear deformations, which is suitable for the analysis of thin/moderately thick anisotropic laminated cylindrical shells under any arbitrary loadings, is developed here.

HIGHER-ORDER THEORIES FOR COMPOSITE LAMINATES

The development of the present theory is based on the following displacement model:

$$U_i = u_i + z\theta_i + z^2 u_i^* + z^3\theta_i^*, \quad (i = 1, 2)$$
$$U_3 = u_3 \tag{1}$$

in which the functions U_i $(i = 1, 3)$ are defined in space at a distance z with reference to a curvilinear surface. The mid-surface of the shell is treated as this reference surface. The remaining functions (u_1, u_2, u_3) and (θ_1, θ_2) are the reference surface displacement components and rotations respectively, whereas u_i^* and θ_i^* $(i = 1, 2)$ are the corresponding higher-order terms of the Taylor's series expansion [6] and are defined at the reference surface only. These are two-dimensional quantities. Equation (1) contains the minimum number of terms to include the effects of transverse shear deformation with warping of the transverse normal cross-section. Thus the generalized displacement vector $\boldsymbol{\delta}^s$ of the reference surface in the shell coordinates consists of

$$\boldsymbol{\delta}^s = (u_1, u_2, u_3, \theta_1, \theta_2, u_1^*, u_2^*, \theta_1^*, \theta_2^*)^t. \tag{2}$$

By substituting eqn (1) into the strain–displacement equations (see Kraus [11], Kant [6]) and reducing it for a cylindrical shell, the physical strain components are derived. In the present work, two theories have been developed: (1) a *Geometrically Thin Shell Theory*, in which the ratio of the thickness to radius of curvature is negligible compared to unity, i.e. $h/R \ll 1$ and (2) a *Geometrically Thick Shell Theory*, in which the square of the ratio is negligible as compared to unity, i.e. $(h/R)^2 \ll 1$, where h and R are thickness and radius respectively. The strain components, thus, for the two theories are given as follows.

Geometrically thin shell:

$$\epsilon_i^z = (\epsilon_i + z\kappa_i + z^2\epsilon_i^* + z^3\kappa_i^*), \quad (i = 1, 2)$$
$$\gamma_{12}^z = (\epsilon_{12} + z\kappa_{12} + z^2\epsilon_{12}^* + z^3\kappa_{12}^*)$$
$$\gamma_{i3}^z = (\phi_i + z\psi_i + z^2\phi_i^*), \quad (i = 1, 2). \tag{3a}$$

The 18 new functions appearing in eqn (3a) form the generalized strain vector $\bar{\boldsymbol{\epsilon}}$ of the reference surface and are related to the generalized displacement vector $\boldsymbol{\delta}^s$ by the following matrix relation:

$$\bar{\boldsymbol{\epsilon}} = \underline{L}^s\boldsymbol{\delta}^s \tag{3b}$$

in which

$$\bar{\boldsymbol{\epsilon}} = (\epsilon_1, \epsilon_2, \epsilon_{12}, \epsilon_1^*, \epsilon_2^*, \epsilon_{12}^*, \kappa_1, \kappa_2, \kappa_{12}, \kappa_1^*, \kappa_2^*, \kappa_{12}^*, \phi_2, \phi_1, \phi_2^*, \phi_1^*, \psi_2, \psi_1)^t \tag{3c}$$

and $\underline{L}^s$ is a differential operator matrix of size 18×9 and its non-zero elements for a cylindrical shell are obtained by substituting eqn (1) in the strain–displacement equation (refer to Appendix A).

Similarly for a geometrically thick shell:

$$\epsilon_{\bar{1}} = (\epsilon_1 + z\kappa_1 + z^2\epsilon_1^* + z^3\kappa_1^*)/(1 + z/R)$$

$$\epsilon_{\bar{2}} = (\epsilon_2 + z\kappa_2 + z^2\epsilon_2^* + z^3\kappa_2^*)$$

$$\gamma_{\bar{1}\bar{2}} = (\epsilon_{12} + z\kappa_{12} + z^2\epsilon_{12}^* + z^3\kappa_{12}^*)/(1 + z/R) + (\epsilon_{21} + z\kappa_{21} + z^2\epsilon_{21}^* + z^3\kappa_{21}^*)$$

$$\gamma_{\bar{2}\bar{3}} = (\phi_2 + z\psi_2 + z^2\phi_2^*)/(1 + z/R)$$

$$\gamma_{\bar{1}\bar{3}} = (\phi_1 + z\psi_1 + z^2\phi_1^* + z^3\psi_1^*). \tag{4a}$$

The 23 new functions appearing in eqn (4a) form the generalized strain vector $\bar{\epsilon}$ of the reference surface and are related to the generalized displacement vector $\boldsymbol{\delta}^s$ by the following matrix relation:

$$\bar{\epsilon} = \underline{F}^s \boldsymbol{\delta}^s \tag{4b}$$

in which

$$\bar{\epsilon} = (\epsilon_1, \epsilon_2, \epsilon_{12}, \epsilon_{21}, \epsilon_1^*, \epsilon_2^*, \epsilon_{12}^*, \epsilon_{21}^*, \kappa_1, \kappa_2, \kappa_{12}, \kappa_{21}, \kappa_1^*, \kappa_2^*, \kappa_{12}^*, \kappa_{21}^*, \phi_2, \phi_1, \phi_2^*, \phi_1^*, \psi_2, \psi_1, \psi_1^*)^t \tag{4c}$$

and $\underline{F}^s$, like $\underline{L}^s$, is a differential operator matrix of size 23×9 for a geometrically thick shell theory and its non-zero elements for a cylindrical shell are obtained by substituting eqn (1) in the strain–displacement equation (refer to Appendix A).

The stress–strain relationship for the Lth layer (lamina) of the composite has the following form.

$$\begin{Bmatrix} \sigma_1 \\ \sigma_2 \\ \tau_{12} \\ \tau_{23} \\ \tau_{13} \end{Bmatrix}_L = \begin{bmatrix} Q_{11}^L & Q_{12}^L & Q_{13}^L & & \\ Q_{21}^L & Q_{22}^L & Q_{23}^L & & \\ Q_{31}^L & Q_{32}^L & Q_{33}^L & & \\ & & & Q_{44}^L & Q_{45}^L \\ & & & Q_{54}^L & Q_{55}^L \end{bmatrix} \begin{Bmatrix} \epsilon_1 \\ \epsilon_2 \\ \gamma_{12} \\ \gamma_{23} \\ \gamma_{13} \end{Bmatrix}_L. \tag{5a}$$

This is written in a compact form as

$$\boldsymbol{\sigma} = \underline{Q}\boldsymbol{\epsilon} \tag{5b}$$

where $\boldsymbol{\sigma}$ and $\boldsymbol{\epsilon}$ are the stresses and the strains with respect to the cylindrical axes as shown in Fig. 1. The stiffness matrix $\underline{Q}$ with respect to shell coordinates is obtained by transforming the stiffness matrix $\underline{C}$ in the principal material coordinates (1′-2′-3′) to shell co-ordinates (1-2-3) using coordinate transformation matrix [12]. This is given by the relation

$$\underline{Q} = [T^{-1}][C][T^{-1}]^t. \tag{5c}$$

The elements of matrices $\underline{C}$ and $\underline{Q}$ are defined in Appendix B.

The total potential energy π of the system could be written as

$$\Pi = \frac{1}{2}\int_V \boldsymbol{\epsilon}^t\boldsymbol{\sigma}\, \mathrm{d}V - \int_A (\boldsymbol{\delta}^s)^t q\, \mathrm{d}A$$

$$= \frac{1}{2}\int_A \left(\int \boldsymbol{\epsilon}^t\boldsymbol{\sigma}\, \mathrm{d}z\right)\mathrm{d}A - \int_A (\boldsymbol{\delta}^s)^t q\, \mathrm{d}A. \tag{6a}$$

By introducing the stress resultants and couples, which are obtained by integrating the physical stress components through the shell thickness in eqn (6a), defined per unit arc length of the reference surface of the shell, the potential energy of the system can be written as

$$\Pi = \frac{1}{2}\int_A \bar{\boldsymbol{\epsilon}}^t\bar{\boldsymbol{\sigma}}\, \mathrm{d}A - \int_A (\boldsymbol{\delta}^s)^t\mathbf{q}\, \mathrm{d}A. \tag{6b}$$

The components of the stress resultant vector $\bar{\boldsymbol{\sigma}}$ are as follows for geometrically thin and thick shell theories.

Geometrically thin shell ($h/R \ll 1$):

$$\begin{bmatrix} N_1 & N_1^* \\ N_2 & N_2^* \\ N_{12} & N_{12}^* \end{bmatrix} = \sum_{L=1}^{NL}\int_{h_L}^{h_{L+1}} \begin{bmatrix} \sigma_1 \\ \sigma_2 \\ \tau_{12} \end{bmatrix} [1, z^2]\, \mathrm{d}z$$

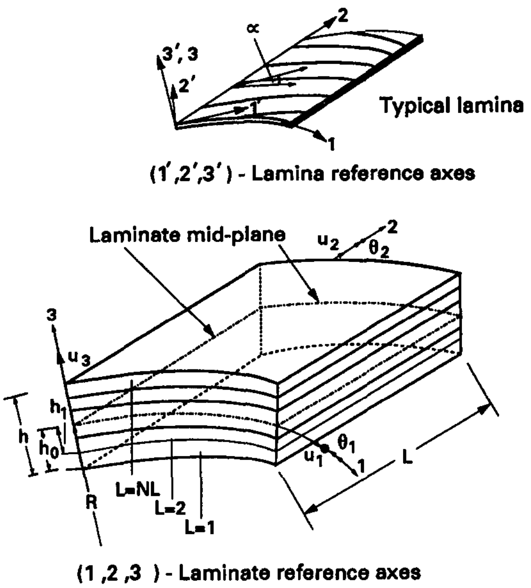

Fig. 1. Laminate geometry with positive set of lamina/laminate axis, displacement components and fibre orientation.

$$\begin{bmatrix} M_1 & M_1^* \\ M_2 & M_2^* \\ M_{12} & M_{12}^* \end{bmatrix} = \sum_{L=1}^{NL} \int_{h_L}^{h_{L+1}} \begin{bmatrix} \sigma_1 \\ \sigma_2 \\ \tau_{12} \end{bmatrix} [z, z^3]\,dz$$

$$\begin{bmatrix} Q_2 & Q_2^* \\ Q_1 & Q_1^* \end{bmatrix} = \sum_{L=1}^{NL} \int_{h_L}^{h_{L+1}} \begin{bmatrix} \tau_{23} \\ \tau_{13} \end{bmatrix} [1, z^2]\,dz$$

$$\begin{bmatrix} S_2 \\ S_1 \end{bmatrix} = \sum_{L=1}^{NL} \int_{h_L}^{h_{L+1}} \begin{bmatrix} \tau_{23} \\ \tau_{13} \end{bmatrix} z\,dz. \tag{7a}$$

Geometrically thick shell $[(h/R)^2 \ll 1]$:

$$\begin{bmatrix} N_1 & N_1^* \\ N_2 & N_2^* \\ N_{12} & N_{12}^* \\ N_{21} & N_{21}^* \end{bmatrix} = \sum_{L=1}^{NL} \times \int_{h_L}^{h_{L+1}} \begin{bmatrix} 1 & 0 & 0 & 0 \\ 0 & A & 0 & 0 \\ 0 & 0 & 1 & 0 \\ 0 & 0 & 0 & A \end{bmatrix} \begin{bmatrix} \sigma_1 \\ \sigma_2 \\ \tau_{12} \\ \tau_{21} \end{bmatrix} [1, z^2]\,dz$$

$$\begin{bmatrix} M_1 & M_1^* \\ M_2 & M_2^* \\ M_{12} & M_{12}^* \\ M_{21} & M_{21}^* \end{bmatrix} = \sum_{L=1}^{NL} \times \int_{h_L}^{h_{L+1}} \begin{bmatrix} 1 & 0 & 0 & 0 \\ 0 & A & 0 & 0 \\ 0 & 0 & 1 & 0 \\ 0 & 0 & 0 & A \end{bmatrix} \begin{bmatrix} \sigma_1 \\ \sigma_2 \\ \tau_{12} \\ \tau_{21} \end{bmatrix} [z, z^3]\,dz$$

$$\begin{bmatrix} Q_2 & Q_2^* \\ Q_1 & Q_1^* \end{bmatrix} = \sum_{L=1}^{NL} \int_{h_L}^{h_{L+1}} \begin{bmatrix} A & 0 \\ 0 & 1 \end{bmatrix} \begin{bmatrix} \tau_{23} \\ \tau_{13} \end{bmatrix} [1, z^2]\,dz$$

$$S_2 = \sum_{L=1}^{NL} \int_{h_L}^{h_{L+1}} \tau_{23} A z\,dz$$

$$[S_1 \quad S_1^*] = \sum_{L=1}^{NL} \int_{h_L}^{h_{L+1}} \tau_{13}[z, z^3]\,dz, \tag{7b}$$

where $A = (1 + z/R)$ and NL is the number of layers.

Thus by substituting eqn (5) in eqns (7a, b), for geometrically thin shell and thick shell theories respectively, and using eqns (3b) and (4b), we get the constitutive relationship for the shell, which is as follows.

$$\begin{bmatrix} \mathbf{N} \\ \mathbf{N}^* \\ \hdashline \mathbf{M} \\ \mathbf{M}^* \\ \hdashline \mathbf{Q} \\ \mathbf{Q}^* \end{bmatrix} = \begin{bmatrix} D_M & D_C & 0 \\ \hdashline D_C' & D_B & 0 \\ \hdashline 0 & 0 & D_S \end{bmatrix} \begin{bmatrix} \boldsymbol{\epsilon}_0 \\ \boldsymbol{\epsilon}_0^* \\ \hdashline \boldsymbol{\kappa}_0 \\ \boldsymbol{\kappa}_0^* \\ \hdashline \boldsymbol{\phi}_0 \\ \boldsymbol{\phi}_0^* \end{bmatrix} \tag{8a}$$

or

$$\bar{\sigma} = \underline{D}\bar{\epsilon} \tag{8b}$$

in which

$$\begin{aligned} &\mathbf{N} = (N_1, N_2, N_{12})'; && \mathbf{N}^* = (N_1^*, N_2^*, N_{12}^*)' \\ &\mathbf{M} = (M_1, M^2, M_{12})'; && \mathbf{M}^* = (M_1^*, M_2^*, M_{12}^*)' \\ &\mathbf{Q} = (Q_2, Q_1)'; && \mathbf{Q}^* = (Q_2^*, Q_1^*, S_2, S_1)' \\ &\boldsymbol{\epsilon}_0 = (\epsilon_1, \epsilon_2, \epsilon_{12})'; && \boldsymbol{\epsilon}_0^* = (\epsilon_1^*, \epsilon_2^*, \epsilon_{12}^*)' \\ &\boldsymbol{\kappa}_0 = (\kappa_1, \kappa_2, \kappa_{12})'; && \boldsymbol{\kappa}_0^* = (\kappa_1^*, \kappa_2^*, \kappa_{12}^*)' \\ &\boldsymbol{\phi}_0 = (\phi_2, \phi_1)'; && \boldsymbol{\phi}_0^* = (\phi_2^*, \phi_1^*, \psi_2, \psi_1)' \end{aligned} \tag{8c}$$

for geometrically thin shell theory, and

$$\begin{aligned} &\mathbf{N} = (N_1, N_2, N_{12}, N_{21})'; && \mathbf{N}^* = (N_1^*, N_2^*, N_{12}^*, N_{21}^*)' \\ &\mathbf{M} = (M_1, M_2, M_{12}, M_{21})'; && \mathbf{M}^* = (M_1^*, M_2^*, M_{12}^*, M_{21}^*)' \\ &\mathbf{Q} = (Q_2, Q_1)'; && \mathbf{Q}^* = (Q_2^*, Q_1^*, S_2, S_1, S_1^*)' \\ &\boldsymbol{\epsilon}_0 = (\epsilon_1, \epsilon_2, \epsilon_{12}, \epsilon_{21})'; && \boldsymbol{\epsilon}_0^* = (\epsilon_1^*, \epsilon_2^*, \epsilon_{12}^*, \epsilon_{21}^*)' \\ &\boldsymbol{\kappa}_0 = (\kappa_1, \kappa_2, \kappa_{12}, \kappa_{21})'; && \boldsymbol{\kappa}_0^* = (\kappa_1^*, \kappa_2^*, \kappa_{12}^*, \kappa_{21}^*)' \\ &\boldsymbol{\phi}_0 = (\phi_2, \phi_1)'; && \boldsymbol{\phi}_0^* = (\phi_2^*, \phi_1^*, \psi_2, \psi_1, \psi_1^*)' \end{aligned} \tag{8d}$$

for geometrically thick shell theory. The individual sub-matrices of the rigidity matrix D are

$\underline{D}_M$—membrane rigidity matrix

$\underline{D}_C$—membrane-flexure coupling matrix

$\underline{D}_B$—flexure rigidity matrix

$\underline{D}_S$—shear rigidity matrix.

The elements in each of the above mentioned sub-matrices are defined in Appendix C and Appendix D, for the geometrically thin and thick shell theories respectively.

FINITE ELEMENT DISCRETIZATION

We follow the standard finite element discretization procedure in which the total domain Ω is subdivided into NE sub-domains or elements such that the total potential energy of the system can be expressed in terms of the potential energies of the elements given by the expression

$$\Pi(\boldsymbol{\delta}) = \sum_{e=1}^{NE} \Pi^e(\boldsymbol{\delta}^s) \tag{9}$$

where Π and Π^e are the potential energies of the system and the element respectively. We further have

$$\Pi^e(\boldsymbol{\delta}^s) = \mathsf{U}^e - \mathbb{W}^e \tag{10}$$

in which U^e and $\mathbb{W}^e$ are the internal strain energy and the external work done respectively. Thus the total potential energy of the system can be written as follows.

$$\Pi(\boldsymbol{\delta}^s) = \sum_{e=1}^{NE} \left\{ \int_A \bar{\epsilon}^t \bar{\sigma} \, dA - \int_A (\boldsymbol{\delta}^s)^t q \, dA \right\}. \tag{11}$$

It can be seen that the potential energy given by the above expression contains only the first derivatives of the elements in $\boldsymbol{\delta}^s$ and thus only C^0 continuity is required for the shape functions to be used in the element formulations. In the C^0 finite element theory, the continuum displacement vector within the element is discretized such that

$$\boldsymbol{\delta}^s = \sum_{i=1}^{NN} N_i(\theta, x) \boldsymbol{\delta}_i^s \tag{12}$$

where $N_i(\theta, x)$ is the interpolating or shape functions associated with node i, $\boldsymbol{\delta}_i^s$ is the displacement vector corresponding to node i, and NN is the number of nodes per element. Equation (11) ensures that the displacement vector $\boldsymbol{\delta}^s$ is not only continuous within the element but over the entire domain since the same value of $\boldsymbol{\delta}^s$ is used for all the elements at the common nodes. Thus C^0 formulation makes the relation (9) a true one. For more details, reference may be made to Zienkiewicz [13], Cook [14], Chaudhary [15], Kant *et al.* [16], Kant [17], etc.

To avoid membrane/shear locking, a phenomenon quite well-known with C^0 formulations of shear-deformation theory, the contributions to the stiffness terms are evaluated in parts—membrane, flexure and shear. The contribution of the individuals to the stiffness terms are evaluated using the selective integration technique. There exists an extensive literature on this selective integration technique (see e.g. Kant and Kulkarni [18], Malkus and Hughes [19]).

In the present work, a four-noded bilinear and a nine-noded quadrilateral element from the Langragian family and an eight-noded quadrilateral element from the Serendipity family have been used along with isoparametric formulation.

NUMERICAL EXAMPLES

A computer programme incorporating existing higher-order theories is developed for the analysis of composite cylindrical shells. Unless stated otherwise, in all numerical examples, a quarter shell is discretized with two or three elements in the circumferential direction and eight elements in the meridional direction. In the case of cylindrical tanks with the same boundary conditions at the opposite ends, only half of the tank is considered for the discretization. The selective integration scheme, namely $3 \times 3 \times 2$, has been employed for the contributions of membrane, flexure and shear to the element stiffness. The displacements and the stress-resultants are presented in non-dimensional form using the multiplier as defined in the respective examples such that

Non-dimensional radial displacement
$= m_1 \times$ actual displacement

Non-dimensional circumferential force
$= m_2 \times$ actual circumferential force

Non-dimensional meridional moments
$= m_3 \times$ actual meridional moment

Non-dimensional circumferential moments
$= m_4 \times$ actual circumferential moment

Non-dimensional transverse shear
$= m_5 \times$ actual transverse shear.

Example 1

An isotropic cylindrical shell, fixed at the ends and subjected to uniform internal pressure (p_0) = 1 kg/cm^2 is analysed for various radius-to-thickness ratios (R/t = 5, 10 and 20). The uniform pressure is assumed to be acting on the mid-surface in geometrically thin shell theory and on the inner surface in geometrically thick shell theory. The material properties are $E = 2.1 \times 10^5$ kg/cm^2 and $\mu = 0.1$. The length of the shell L = 800 cm and radius R = 200 cm [Fig. 5(a)]. The various non-dimensional multipliers are given as

$$m_1 = \frac{Eh}{p_0 R^2}; \quad m_2 = \frac{1}{p_0 R}; \quad m_3 = \frac{4}{p_0 Rh}; \quad m_4 = \frac{4}{\mu p_0 Rh}.$$

Their variations along the length of the cylinder are shown in Figs 2(a–l), and are compared with values obtained by Kant [6].

Example 2

A cantilever cylinder subjected to a uniform radial shear (P) = 1 lb/in. at the free end is considered. The material properties and size of the cylinder are as follows. $E = 30 \times 10^6$ lb/in^2, $\mu = 0.3$, L = 25 in., R = 10 in. and the thickness h = 2.5 in. [Fig. 5(b)]. The non-dimensional values of the radial displacements and the stress resultants are calculated using the multipliers defined below. Their variations along

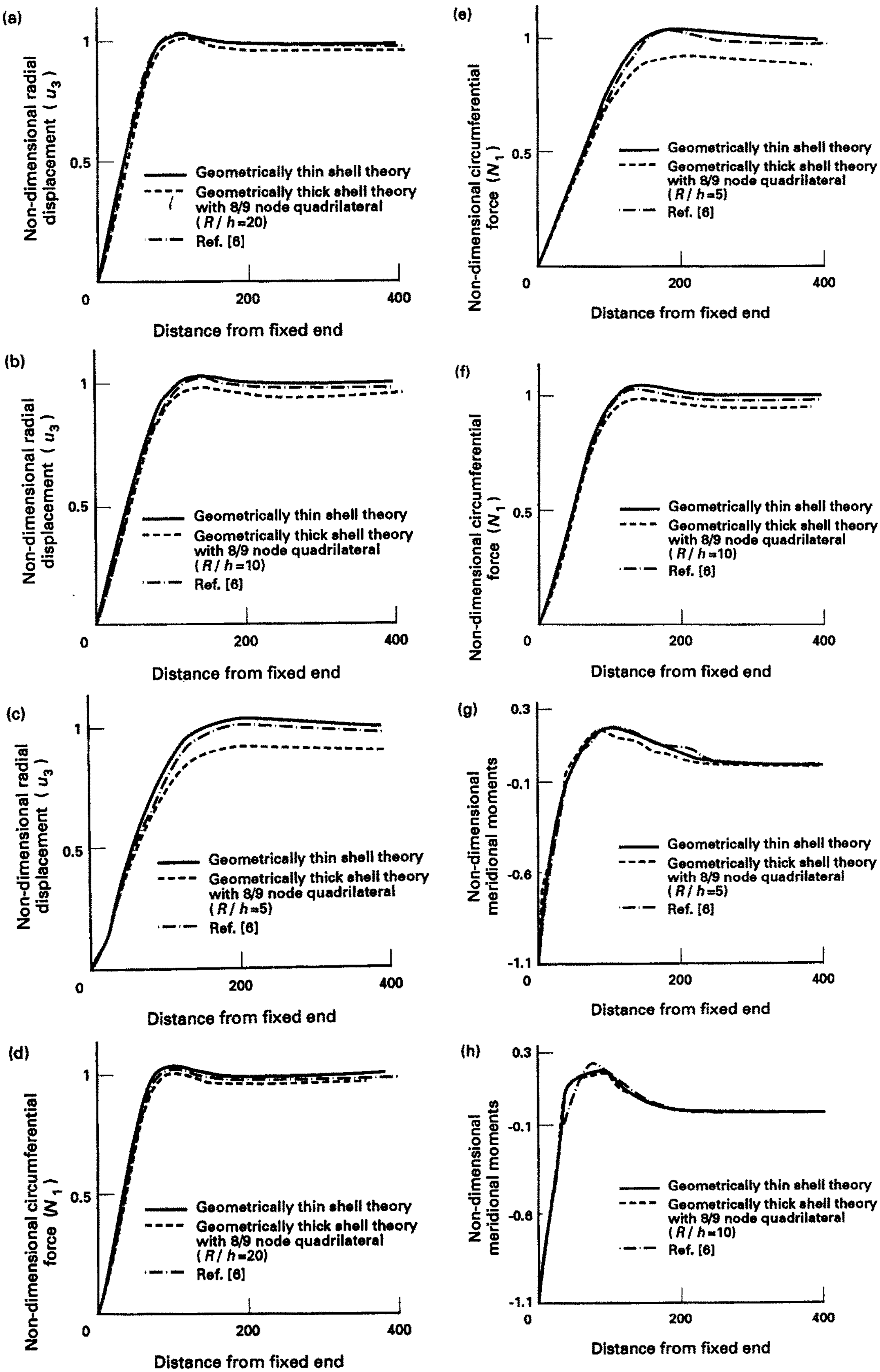
(a)
Non-dimensional radial displacement (u_3)
Geometrically thin shell theory
Geometrically thick shell theory with 8/9 node quadrilateral (R/h=20)
Ref. [6]
Distance from fixed end
(b)
Non-dimensional radial displacement (u_3)
Geometrically thin shell theory
Geometrically thick shell theory with 8/9 node quadrilateral (R/h=10)
Ref. [6]
Distance from fixed end
(c)
Non-dimensional radial displacement (u_3)
Geometrically thin shell theory
Geometrically thick shell theory with 8/9 node quadrilateral (R/h=5)
Ref. [6]
Distance from fixed end
(d)
Non-dimensional circumferential force (N_1)
Geometrically thin shell theory
Geometrically thick shell theory with 8/9 node quadrilateral (R/h=20)
Ref. [6]
Distance from fixed end
(e)
Non-dimensional circumferential force (N_1)
Geometrically thin shell theory
Geometrically thick shell theory with 8/9 node quadrilateral (R/h=5)
Ref. [6]
Distance from fixed end
(f)
Non-dimensional circumferential force (N_1)
Geometrically thin shell theory
Geometrically thick shell theory with 8/9 node quadrilateral (R/h=10)
Ref. [6]
Distance from fixed end
(g)
Non-dimensional meridional moments
Geometrically thin shell theory
Geometrically thick shell theory with 8/9 node quadrilateral (R/h=5)
Ref. [6]
Distance from fixed end
(h)
Non-dimensional meridional moments
Geometrically thin shell theory
Geometrically thick shell theory with 8/9 node quadrilateral (R/h=10)
Ref. [6]
Distance from fixed end

Fig. 2(a–h)

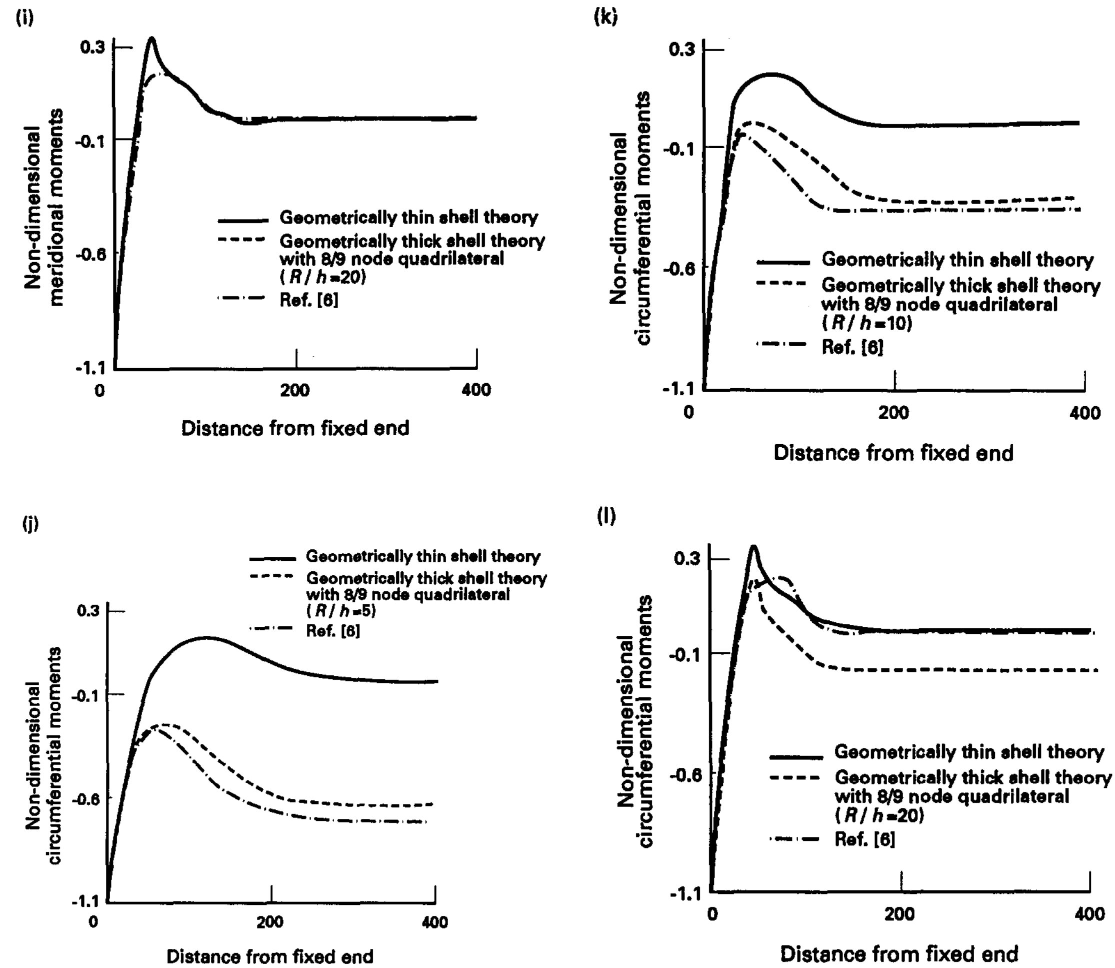

Fig. 2(i–l)

Fig. 2. (a) Variation of radial displacement along the length of the cylinder, for $R/h = 20$, (b) for $R/h = 10$, (c) for $R/h = 5$. (d) Variation of circumferential force along the length of the cylinder, for $R/h = 20$, (e) for $R/h = 5$, (f) for $R/h = 10$. (g) Variation of meridional moments along the length of the cylinder, for $R/h = 5$, (h) for $R/h = 10$, (i) for $R/h = 20$. (j) Variation of circumferential moments along the length of the cylinder, for $R/h = 5$, (k) for $R/h = 10$, (l) for $R/h = 20$.

the length are shown in Fig. 3(a–d).

$$m_1 = \frac{Eh\sqrt{Rh}}{PR^2}; \quad m_2 = \frac{\sqrt{Rh}}{PR};$$

$$m_3 = \frac{4\sqrt{Rh}}{PRh}; \quad M_4 = \frac{4\sqrt{Rh}}{\mu PRh}.$$

Example 3

A cylinder fixed at the ends, made up of orthotropic material subjected to an internal pressure $p_0 = 1\ \text{kg/cm}^2$ is analysed [Fig. 5(a)]. The material properties and geometry of the shell are defined as follows [6].

$$C_{22} = 2.1 \times 10^5\ \text{kg/cm}^2 \qquad C_{33} = 0.262931 \times C_{22}\ \text{kg/cm}^2$$

$$C_{11} = 0.543103 \times C_{22}\ \text{kg/cm}^2 \qquad C_{44} = 0.159914 \times C_{22}\ \text{kg/cm}^2$$

$$C_{12} = 0.233190 \times C_{22}\ \text{kg/cm}^2 \qquad C_{55} = 0.266810 \times C_{22}\ \text{kg/cm}^2$$

$L = 800\ \text{cm}$, $R = 200\ \text{cm}$,

thickness $h = 40$, 20 and 10 cm.

The variations of non-dimensionalized radial displacement and stress resultant along the length of the shell have been presented in Fig. 4(a–l), using the multipliers defined below. The maximum values of these quantities are presented in Table 1.

$$m_1 = \frac{E_{11}h}{p_0 R^2}; \quad m_2 = \frac{1}{p_0 R}; \quad m_3 = \frac{4}{p_0 Rh};$$

$$m_4 = \frac{16}{p_0 Rh}; \quad m_5 = \frac{1}{p_0\sqrt{Rh}}.$$

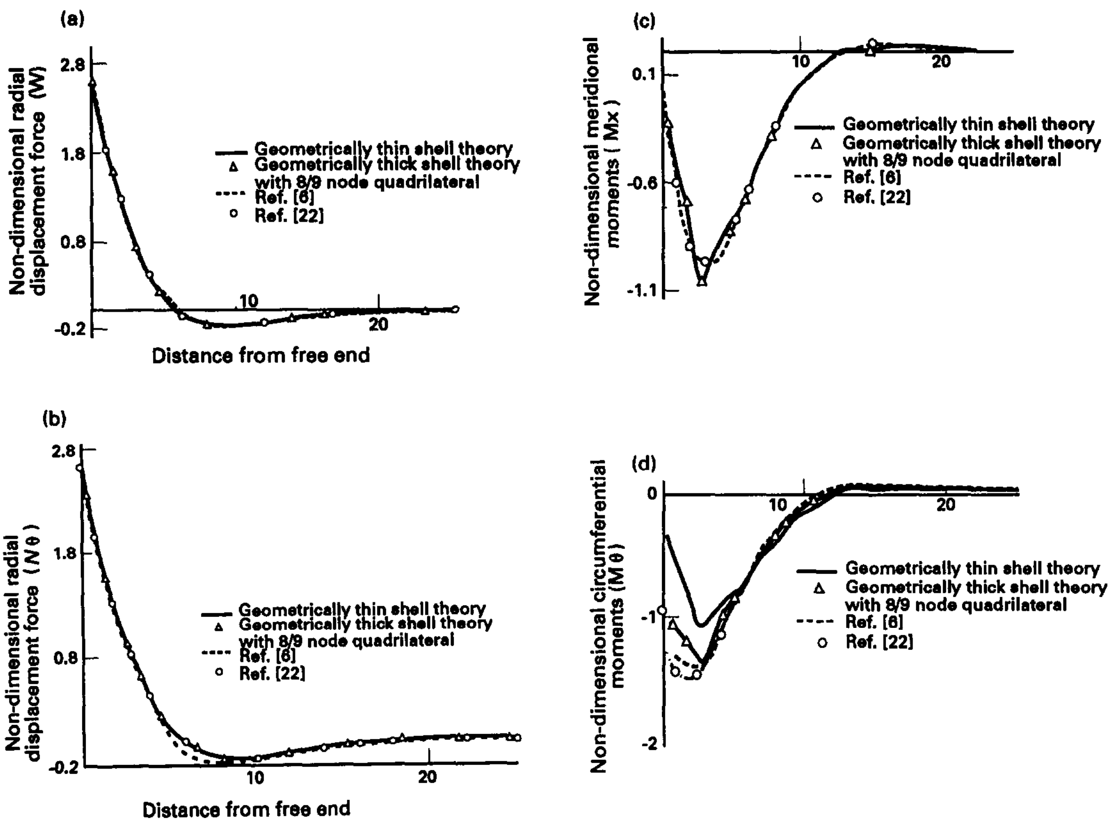

Fig. 3. (a) Variation of radial displacement along the length of the cylinder. (b) Variation of circumferential force along the length of the cylinder. (c) Variation of meridional moments along the length of the cylinder. (d) Variation of circumferential moments along the length of the cylinder.

Example 4

A fixed cylindrical shell made up of four-layered angle-ply, (45°/−45°/−45°/45°) and (0°/90°/90°/0°), of equal thickness and subjected to internal pressure of $p_0 = (6.41/\pi)$ psi is considered. The material properties of the fibres are given by [20], as follows. $E_1 = 7.5 \times 10^6$ psi, $E_2 = 2.0 \times 10^6$ psi, $G_{12} = 1.25 \times 10^6$ psi, $G_{23} = 0.63 \times 10^6$ psi $= G_{13}$ and $\mu_{12} = 0.25$. The general shape of the tank is defined as $L = 20$ in., $R = 20$ in. and $h = 1.0$ and 0.20 in. [Fig. 5(a)].

Table 2 gives the maximum value of the normal displacement at the centre of the cylindrical shell.

Table 1. Maximum values of displacement and stress resultants in Example 3

$\frac{R}{h}$	Theories	Non-dimensional form of dependent variables $u_3 \times m_1$	$N_1 \times m_2$	$M_2 \times m_3$	$M_1 \times m_4$	$Q_2 \times m_5$
5	Geom. thin	1.049	1.025	−1.092	−1.050	0.675
	Geom. thick	0.947	0.925	−1.020	−0.960	0.602
	Ref. [6]	1.061	1.030	−1.216	−1.150	0.704
10	Geom. thin	0.998	1.032	−1.163	−1.090	0.722
	Geom. thick	1.049	0.980	−1.095	−1.070	0.682
	Ref. [6]	1.089	1.035	−1.351	−1.200	0.750
20	Geom. thin	1.024	1.037	−1.131	−1.056	0.732
	Geom. thick	1.049	1.013	−1.100	−1.024	0.712
	Ref. [6]	1.086	1.035	−1.430	−1.200	0.800

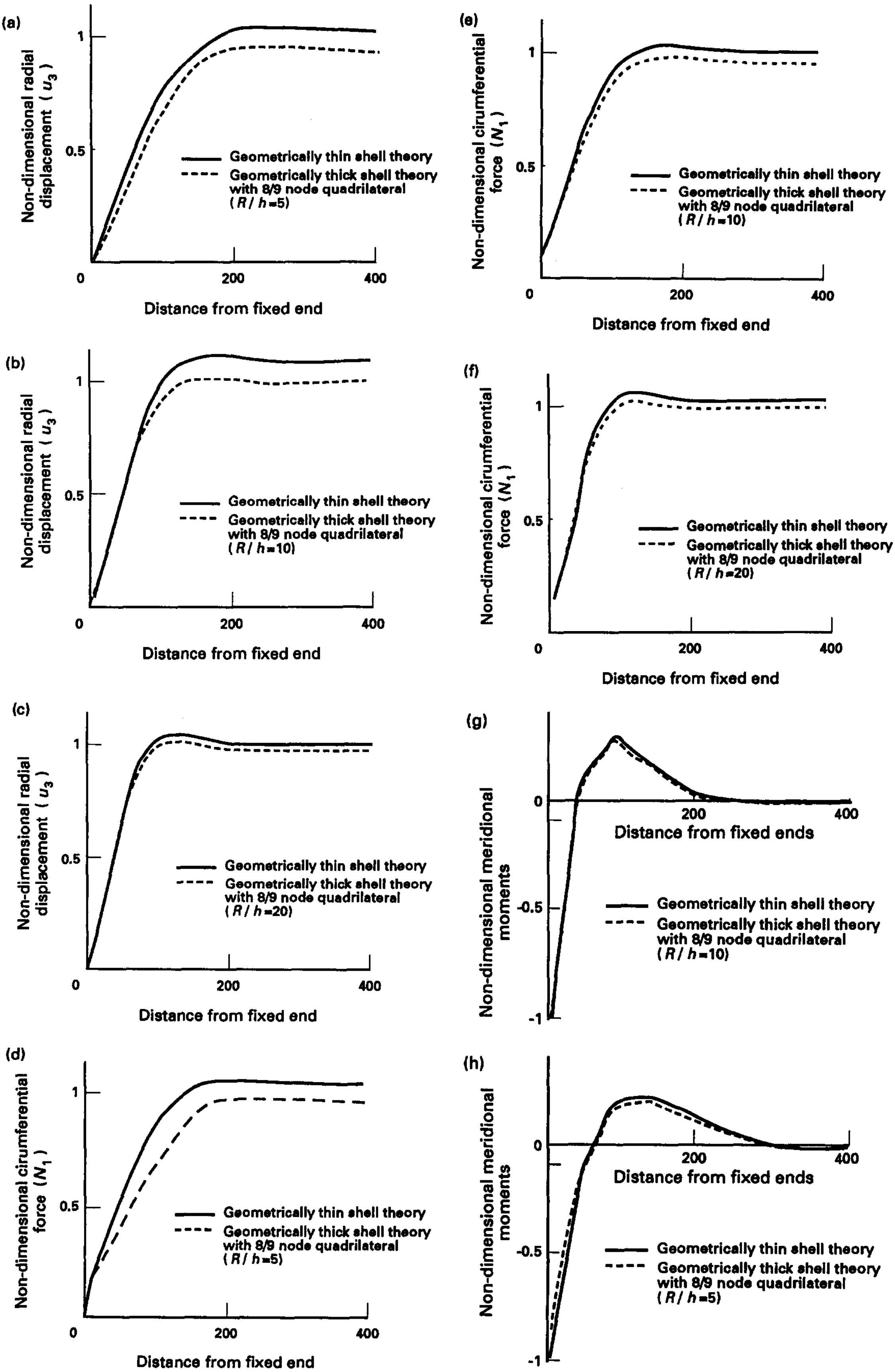
(a)
Non-dimensional radial displacement (u_3)
1
0.5
0
200
400
Distance from fixed end
Geometrically thin shell theory
Geometrically thick shell theory with 8/9 node quadrilateral (R / h = 5)
(b)
Non-dimensional radial displacement (u_3)
1
0.5
0
200
400
Distance from fixed end
Geometrically thin shell theory
Geometrically thick shell theory with 8/9 node quadrilateral (R / h = 10)
(c)
Non-dimensional radial displacement (u_3)
1
0.5
0
200
400
Distance from fixed end
Geometrically thin shell theory
Geometrically thick shell theory with 8/9 node quadrilateral (R / h = 20)
(d)
Non-dimensional cirumferential force (N_1)
1
0.5
0
200
400
Distance from fixed end
Geometrically thin shell theory
Geometrically thick shell theory with 8/9 node quadrilateral (R / h = 5)
(e)
Non-dimensional cirumferential force (N_1)
1
0.5
0
200
400
Distance from fixed end
Geometrically thin shell theory
Geometrically thick shell theory with 8/9 node quadrilateral (R / h = 10)
(f)
Non-dimensional cirumferential force (N_1)
1
0.5
0
200
400
Distance from fixed end
Geometrically thin shell theory
Geometrically thick shell theory with 8/9 node quadrilateral (R / h = 20)
(g)
Non-dimensional meridional moments
0
-0.5
-1
200
400
Distance from fixed ends
Geometrically thin shell theory
Geometrically thick shell theory with 8/9 node quadrilateral (R / h = 10)
(h)
Non-dimensional meridional moments
0
-0.5
-1
200
400
Distance from fixed ends
Geometrically thin shell theory
Geometrically thick shell theory with 8/9 node quadrilateral (R / h = 5)

Fig. 4(a–h)

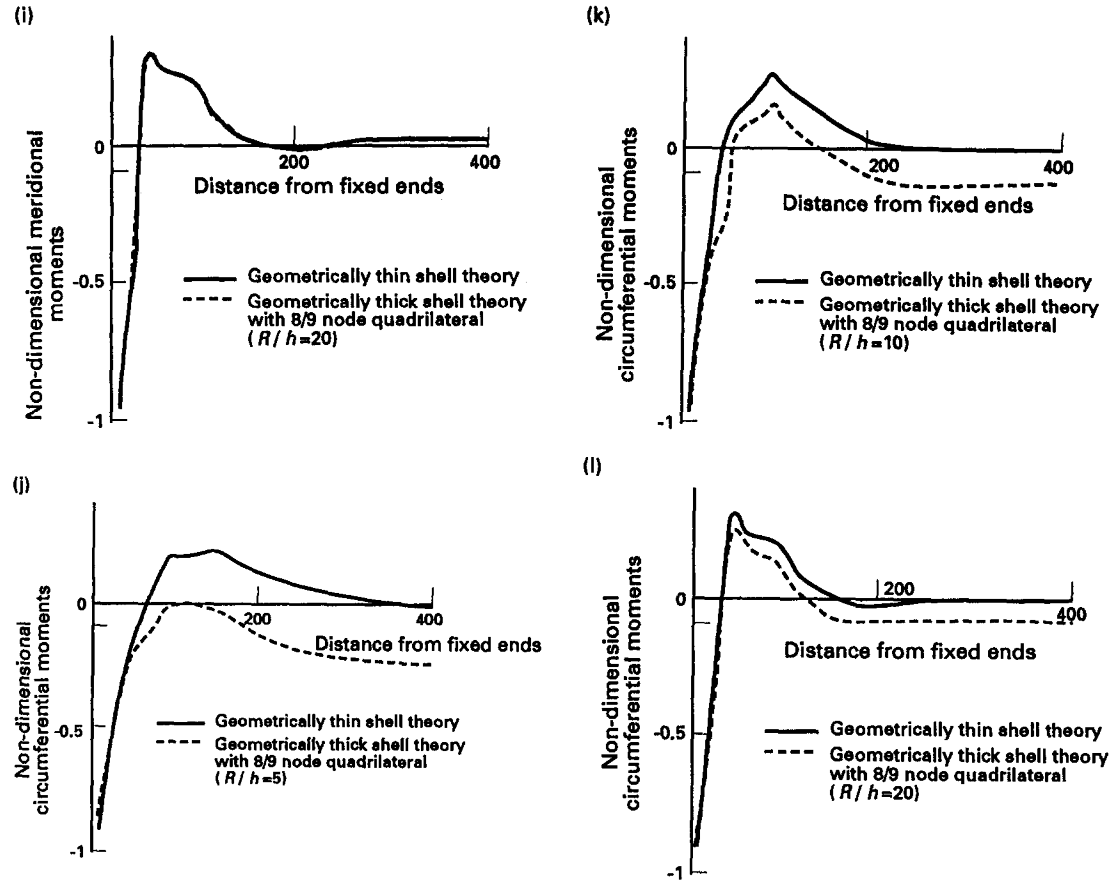

Fig. 4(i–l)

Fig. 4. (a) Variation of radial displacement along the length of the cylinder for $R/h = 5$, (b) for $R/h = 10$, (c) for $R/h = 20$. (d) Variation of circumferential force along the length of the cylinder for $R/h = 5$, (e) for $R/h = 10$, (f) for $R/h = 20$. (g) Variation of meridional moments along the length of the cylinder for $R/h = 10$, (h) for $R/h = 5$, (i) for $R/h = 20$. (j) Variation of circumferential moments along the length of the cylinder for $R/h = 5$, (k) for $R/h = 10$, (l) for $R/h = 20$.

Because of symmetry of the layered shell, only a quarter of the shell was discretized.

Example 5

A 90° cylindrical shell clamped at all the edges and subjected to a uniform pressure of $p_0 = (6.41/\pi)$ psi is considered [Fig. 5(c)] [20]. The different fibre orientations considered are (−45°/45°); (45°/−45°/−45°/45°) and (0°/90°/90°/0°). The material properties and the geometry of the shell are the same as described in Example 4. The problem is solved for different thickness to radius ratios given as $R/h = 20$, 100 and 300, and for each different fibre orientation. The maximum value of radial displacement at the

Table 2. Radial displacements $u_3 \times (E_1 h/P_0 R^2)$ in Example 4

		Thin shell theory			Thick shell theory			Reference[20]	
$\frac{R}{h}$	Fibre Angle	Nine-noded	Eight-noded	Four-noded	Nine-noded	Eight-noded	Four-noded	4 × 4 mesh	6 × 6 mesh
20	(45°/−45° −45°/45°)	2.21	2.21	1.94	2.16	2.16	1.89	2.20	2.21
100	(45°/−45° −45°/45°)	1.95	1.96	1.98	1.94	1.95	1.97	1.97	1.96
20	(0°/90° 90°/0°)	1.67	1.67	1.51	1.63	1.63	1.47	1.64	1.64
100	(0°/90° 90°/0°)	1.55	1.55	1.59	1.55	1.55	1.58	1.55	1.55

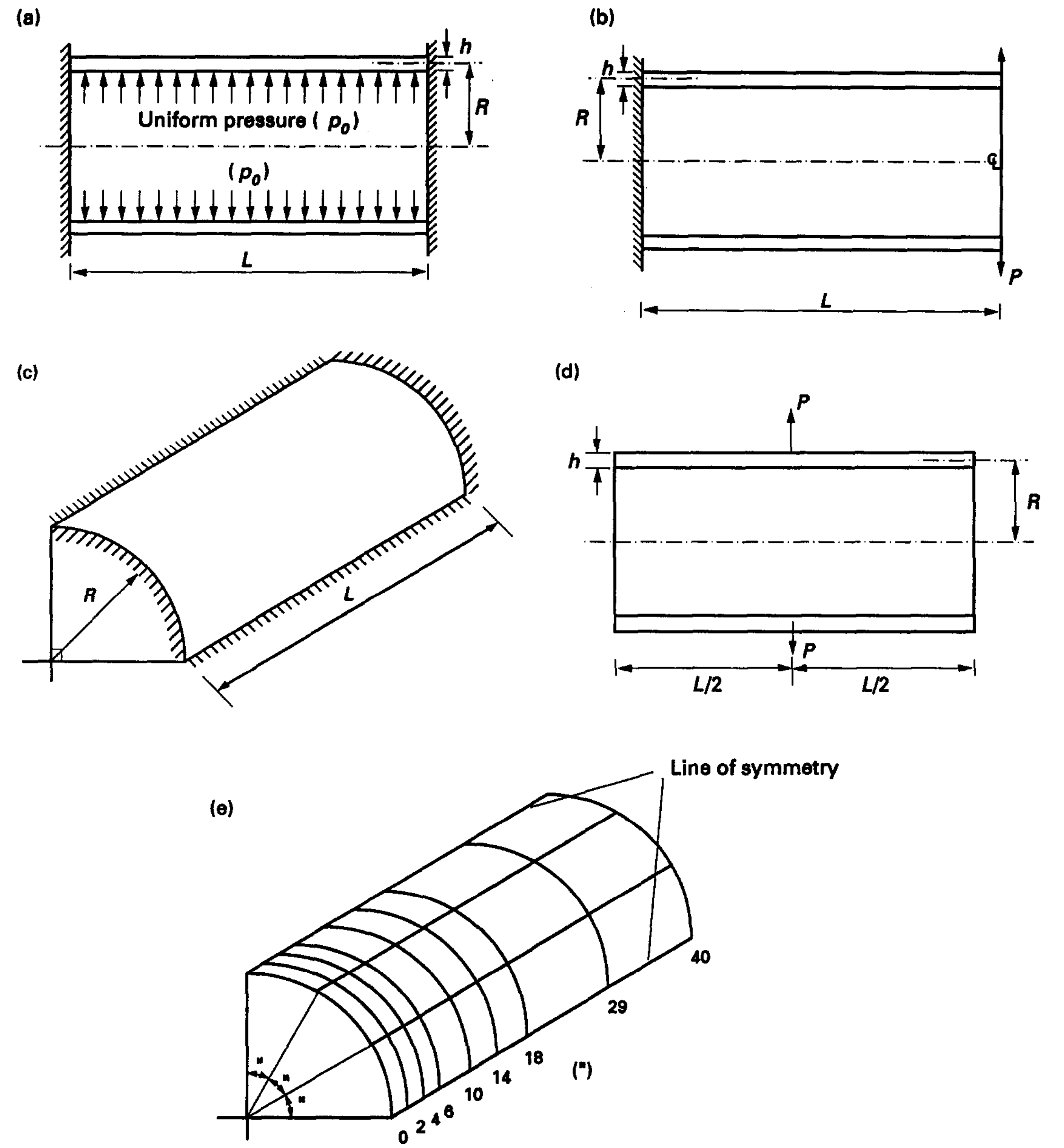

Fig. 5. (a) Cylindrical shell, fixed at the ends and subjected to internal pressure. (b) Cantilever shell subjected to radial shear at free end. (c) 90° cylindrical shell clamped at all the edges and subjected to uniform pressure. (d) Cylindrical shell with free ends under a distributed line load around the central circle. (e) Shell discretization for Example 6.

centre is given in Table 3. Because the problem is non-axisymmetric, the full shell is discretized to get the solution.

Example 6

A sandwich and layered circular cylindrical shell under uniformly distributed line loads of $P = 14417$ lb/in. around a central circle is analysed [21]. The geometry is as follows: length $L = 80$ in., total thickness $h = 2.4$ in., radius $R = 18$ in. [Fig. 5(d)]. The shell is discretized as shown in Fig. 5(e). The material and cross-sectional properties are: (a) three layered sandwich, isotropic shell, thickness of facing $t_f = 0.2$ in., thickness of core $t_c = 2.0$ in., material constants $E_f = 10^7$ psi, $G_f = 3.846 \times 10^6$ psi, $\mu_c = \mu_f = 0.25$, $E_c = 10^5$ psi, $G_c = 3.846 \times 10^4$ psi; (b) cross-ply shell (0°/90°/0°), thickness of each layer $= h/3 = 0.8$ in., material constants $E_1 = 10^7$ psi, $E_2 = 4 \times 10^5$ psi, $G_{12} = 2 \times 10^5$ psi, $G_{13} = G_{23} = 0.8 \times 10^5$ psi; (c) cross-ply shell (90°/0°/90°) has the same properties as in (b). The results are shown in Table 4.

Table 3. Radial displacements $u_3 \times (E_1 h/P_0 R^2)$ in Example 5

$\frac{R}{h}$	Fibre Angle	Thin shell theory Nine-noded	Thin shell theory Eight-noded	Thin shell theory Four-noded	Thick shell theory Nine-noded	Thick shell theory Eight-noded	Thick shell theory Four-noded	Reference[20] 4 × 4 mesh	Reference[20] 6 × 6 mesh
20	−45°/45°	3.51	2.77	1.76	3.42	2.70	1.71	2.68	2.68
100	−45°/45°	2.12	2.05	1.63	2.10	2.04	1.63	1.52	1.64
300	−45°/45°	3.60	2.00	1.62	3.59	2.00	1.62	1.87	2.06
20	(45°/ − 45° −45°/45°)	3.53	2.75	1.77	3.44	2.68	1.72	2.68	2.67
100	(45°/ − 45° −45°/45°)	3.59	2.06	1.63	3.57	2.06	1.62	1.65	1.65
300	(45°/ − 45° −45°/45°)	3.60	2.01	1.62	3.59	2.00	1.62	1.91	2.03
20	(0°/90° 90°/0°)	2.99	2.51	1.50	2.91	2.44	1.47	2.10	2.11
100	(0°/90° 90°/0°)	3.03	1.98	1.44	2.96	1.97	1.42	1.35	1.36
300	(0°/90° 90°/0°)	3.04	1.90	1.43	3.03	1.90	1.43	1.63	1.61

Table 4. Maximum value of stresses and displacement in sandwich and cross-ply (Example 6)

Shell Types	Theories	$u_3 \dfrac{Eh\sqrt{Rh}}{P_0 R^2}$	$N_1 \times \dfrac{\sqrt{RH}}{P_0 R}$	$M_2 \times \dfrac{10}{P_0\sqrt{Rh}}$	$M_1 \times \dfrac{10}{\mu P_0\sqrt{Rh}}$	Remarks
Sandwich isotropic	Geom. thin	5.610	1.040	1.552	−1.678	$E = E_f$
	Geom. thick	5.640	0.990	1.657	−0.580	
	Ref. [21]	7.122	1.206	1.526	−1.452	
	Ref. [23]	6.180	1.128	1.531	−1.531	
Cross-ply (0°/90°/0°)	Geom. thin	3.010	2.009	0.726	−0.596	$E = E_2$
	Geom. thick	3.011	2.008	0.727	−0.681	
	Ref. [21]	2.802	1.534	1.044	−9.760	
Cross-ply (90°/0°/90°)	Geom. thin	3.581	1.199	1.441	−0.056	$E = E_2$
	Geom. thick	3.596	1.199	1.439	−0.063	
	Ref. [21]	3.772	1.194	1.457	−0.095	

CONCLUSIONS

The results from a set of higher-order theories (geometrically thin shell and geometrically thick shell) for a composite and sandwich cylindrical shell subjected to different loadings and end conditions are presented. These theories do not require the usual shear correction coefficients. The results show excellent agreement with the other theories for thin to thick shells. In the case of axisymmetric isotropic, orthotropic, sandwich and cross-ply (symmetrically layered), under axisymmetric loadings, it is observed that eight-noded and nine-noded elements yield the same results.

It is seen from the result shown in Figs 2–4 that both the theories discussed here give the same results in the thin limits and the value is one predicted by the classical Love theory of shells.

The influence of (h/R) ratio in thick shells is quite pronounced. Consistently, the circumferential moment M_1 is the one most affected, while the meridional moment M_2 is less affected. It is also observed that the displacements and membrane stresses for a thick shell do not vary much in these two theories. The slight variation is merely due to the assumption that the loadings act on the mid surface for geometrically thin shell theory and on the inner/outer surface as the case may be for geometrically thick shell theory, which is actually so.

The cross-ply shell shows a drastic redistribution of stresses in the shell due to the layering effect and anisotropy. The results in Table 4 show that the (0°/90°/0°) arrangement is definitely the more efficient one, compared to (90°/0°/90°).

Thus the geometrically thick shell theory should be used for a more reliable and accurate analysis of both thick and thin shells, under any arbitrary loading and boundary conditions.

REFERENCES

1. S. A. Ambartsumyan, *Theory of Anisotropic Shells*. Moscow (1961). English translation, NASA TT F-118, May (1964).

2. S. B. Dong and R. L. Taylor, On the theory of laminated anisotropic shells and plates. *J. Aerospace Sci.* **29,** 969–975 (1962).
3. S. B. Dong and F. K. W. Tso, On a laminated orthotropic shell theory including transverse shear deformation. *J. appl. Mech.* **39,** 1091–1097 (1972).
4. J. M. Whitney and C. T. Sun, A refined theory for laminated anisotropic cylindrical shells. *J. appl. Mech.* **41,** 471–476 (1974).
5. G. E. O. Widera and S. W. Chung, A theory of non-homogeneous anisotropic cylindrical shells. *J. appl. Mech.* **21,** 378–399 (1970).
6. T. Kant, Thick shells of revolution—some studies. Ph.D thesis, Dept. of Civil Engng, I.I.T., Bombay (1976).
7. A. Bhimaraddi, A higher order theory for free vibration analysis of circular cylindrical shells. *Int. J. Solids Struct.* **20,** 623–630 (1984).
8. A. Bhimaraddi and L. K. Stevens, On the higher order theories in plates and shells. *Int. J. Solids Struct.* **6,** 35–50 (1986).
9. C. A. Rogers and C. E. Knight, Jr, An axisymmetric linear/high-order finite element for filament-wound composites—1. Formulation and algorithm. *Comput. Struct.* **29,** 265–271 (1988).
10. A. V. K. Murthy and T. S. R. Reddy, A higher order theory for laminated composite cylindrical shells. *J. Aeronautical Soc. India*, pp. 161–171 (1986).
11. H. Kraus, *Thin Elastic Shells.* John Wiley, New York (1967).
12. B. N. Pandya, Higher order theories and finite element evaluation for multilayered composite plates. Ph.D. thesis, Dept. of Civil Engng, I.I.T., Bombay (1987).
13. O. C. Zienkiewicz, *The Finite Element Method*, 3rd Edn. McGraw–Hill, London (1977).
14. R. D. Cook, *Concept and Applications of Finite Element Analysis*, 2nd Edn. John Wiley, New York (1981).
15. V. P. Chaudhary, Finite element analysis of axisymmetrical shells of composite materials. Ph.D. thesis, Dept. of Engng Mech., University of Nebraska, Lincoln (1970).
16. T. Kant, D. R. J. Owen and O. C. Zienkiewicz, A refined higher order C^0 plate bending element. *Comput. Struct.* **15,** 177–183 (1982).
17. T. Kant, On finite element discretization for a higher order shell theory. In *The Mathematics of Finite Elements and Applications IV* (Edited by J. R. Whiteman), pp. 209–217. Academic Press, London (1982).
18. T. Kant and P. B. Kulkarni, A C^0 continuous linear beam/bilinear plate flexure element. *Comput. Struct.* **22,** 413–425 (1986).
19. D. S. Malkus and T. J. R. Hughes, Mixed finite element method—reduced and selective integration techniques: a unification of concepts. *Comput. Meth. appl. Mech. Engng* **15,** 63–81 (1978).
20. D. J. Hass and S. W. Lee, A nine noded assumed strain finite element method. *Comput. Struct.* **26,** 445–452 (1987).
21. S. G. Ladkany, Five hybrid elements for the analysis of thick, thin or symmetrically layered plates and shells. Ph.D. thesis, Dept. of Civil Engng. Wisconsin University, Madison, WI (1975).
22. M. H. Baluch, Analysis of stress and deformations in moderately thick shell structures. Ph.D. thesis, Purdue University, West Lafayette, IN (1970).
23. F. J. Plantema, *Sandwich Construction.* John Wiley, New York (1966).

APPENDIX A

The non-zero terms of strain displacement matrix $\underset{\sim}{L}^s$ for a geometrically thin shell theory are given as follows.

$$L_{11} = L_{32} = L_{46} = L_{67} = L_{74} = L_{95} = L_{10,8} = L_{12,9} = L_{14,3} = \frac{1\partial}{R\partial\theta}$$

$$L_{22} = L_{31} = L_{57} = L_{66} = L_{85} = L_{94} = L_{11,9} = L_{12,8} = L_{13,3} = \frac{\partial}{\partial x}$$

$$L_{13} = -L_{14,1} = \frac{1}{R};\quad L_{13,5} = L_{14,4} = 1;\quad L_{15,9} = L_{16,8} = 3$$

$$L_{17,7} = L_{18,6} = 2.$$

Similarly, the non-zero terms of strain–displacement matrix $\underset{\sim}{F}^s$ for a geometrically thick shell theory are given as follows.

$$F_{11} = F_{32} = F_{56} = F_{77} = F_{94} = F_{11,5} = F_{13,8} = F_{15,9} = F_{18,3} = \frac{1\partial}{R\partial\theta}$$

$$F_{22} = F_{41} = F_{67} = F_{86} = F_{10,5} = F_{12,4} = F_{14,9} = F_{16,8} = F_{17,3} = \frac{\partial}{\partial x}$$

$$F_{13} = -F_{18,1} = F_{20,6} = \frac{1}{R};\quad F_{17,5} = F_{18,4} = 1$$

$$F_{19,9} = F_{20,8} = 3;\quad F_{21,7} = F_{22,6} = 2;\quad F_{23,8} = \frac{2}{R}.$$

APPENDIX B

$$\underset{\sim}{C} = \begin{bmatrix} C_{11} & C_{12} & 0 & 0 & 0 \\ & C_{22} & 0 & 0 & 0 \\ & & C_{33} & 0 & 0 \\ \text{Symmetric} & & & C_{44} & 0 \\ & & & & C_{55} \end{bmatrix}$$

$$\underset{\sim}{Q} = \begin{bmatrix} Q_{11} & Q_{12} & Q_{13} & 0 & 0 \\ & Q_{22} & Q_{23} & 0 & 0 \\ & & Q_{33} & 0 & 0 \\ \text{Symmetric} & & & Q_{44} & Q_{45} \\ & & & & Q_{55} \end{bmatrix}$$

where the elements of the $\underset{\sim}{C}_{ij}$ matrix are the plane stress reduced elastic constants of Lth lamina and the following relations hold good between these and the engineering elastic constants.

$$C_{11} = \frac{E_{1'}}{1-\nu_{1'2'}\nu_{2'1'}};\quad C_{12} = \frac{\nu_{1'2'}E_{2'}}{1-\nu_{1'2'}\nu_{2'1'}};\quad C_{22} = \frac{E_{2'}}{1-\nu_{1'2'}\nu_{2'1'}}$$

$$C_{33} = G_{1'2'};\quad C_{44} = G_{2'3'};\quad C_{55} = G_{1'3'}$$

and following the usual transformation rule of stresses/tensorial strains between the lamina (1′-2′-3′) and the laminate (1-2-3) coordinate systems, the elements of $\underset{\sim}{Q}_{ij}$ matrix are as follows:

$$Q_{11} = c^4C_{11} + s^4C_{22} + 2\cdot c^2\cdot s^2(C_{12} + 2\cdot C_{33})$$

$$Q_{12} = c^2\cdot s^2(C_{11} + C_{22} - 4\cdot C_{33}) + C_{12}(c^4 + s^4)$$

$$Q_{13} = c^3\cdot s(C_{11} - C_{12} - 2\cdot C_{33}) + c\cdot s^3(C_{12} - C_{22} + 2\cdot C_{33})$$

$$Q_{22} = s^4C_{11} + c^4C_{22} + 2\cdot c^2s^2(C_{12} + 2\cdot C_{33})$$

$$Q_{23} = c \cdot s^3(C_{11} - C_{12} - 2 \cdot C_{33}) + s \cdot c^3(C_{12} - C_{22} + 2 \cdot C_{33})$$

$$Q_{33} = (s^4 + c^4)C_{33} + c^2s^2(C_{11} - 2 \cdot C_{12} + C_{22} - 2 \cdot C_{33})$$

$$Q_{44} = c^2C_{44} + s^2C_{55}; \quad Q_{45} = c \cdot s \cdot (C_{55} - C_{44})$$

$$Q_{55} = s^2C_{44} + c^2C_{55}$$

where, *if* α is the angle between the fibre axis (1′) and laminate axes (1) as shown in Fig. 1, then, $c = \cos\alpha$, $s = \sin\alpha$, $c^2 = \cos^2\alpha$, $s^2 = \sin^2\alpha$ and so on.

APPENDIX C

The elements of $\underset{\sim}{D}$ matrix for a geometrically thin shell theory are given here as follows. If we set

$$H_i = \frac{1}{i}(h^i_{L+1} - h^i_L)$$

such that i takes an integer value between 1 and 7, then the sub-matrix can be readily obtained in the following forms based on the geometrical assumption, $(h/R) \ll 1$.

$$\underset{\sim}{D}_M = \sum_{L=1}^{NL} \begin{bmatrix} H_1Q_{11} & H_1Q_{12} & H_1Q_{13} & H_3Q_{11} & H_3Q_{12} & H_3Q_{13} \\ & H_1Q_{22} & H_1Q_{23} & H_3Q_{21} & H_3Q_{22} & H_3Q_{23} \\ & & H_1Q_{33} & H_3Q_{31} & H_3Q_{32} & H_3Q_{33} \\ & & & H_5Q_{11} & H_5Q_{12} & H_5Q_{13} \\ & & & & H_5Q_{22} & H_5Q_{23} \\ \text{Symmetric} & & & & & H_5Q_{33} \end{bmatrix} L\text{th layer}$$

$$\underset{\sim}{D}_S = \sum_{L=1}^{NL} \begin{bmatrix} H_1Q_{44} & H_1Q_{45} & H_3Q_{44} & H_3Q_{45} & H_2Q_{44} & H_2Q_{45} \\ & H_1Q_{55} & H_3Q_{54} & H_3Q_{55} & H_2Q_{54} & H_2Q_{55} \\ & & H_5Q_{44} & H_5Q_{45} & H_4Q_{44} & H_4Q_{45} \\ & & & H_5Q_{55} & H_4Q_{54} & H_4Q_{55} \\ & & & & H_3Q_{44} & H_3Q_{45} \\ \text{Symmetric} & & & & & H_3Q_{55} \end{bmatrix} L\text{th layer}$$

The elements of the $\underset{\sim}{D}_C$ matrix are obtained by replacing H_1, H_3 and H_5 by H_2, H_4 and H_6 respectively in the $\underset{\sim}{D}_M$ matrix mentioned above. Similarly the $\underset{\sim}{D}_B$ matrix is obtained by replacing H_1, H_3 and H_5 by H_3, H_5 and H_7 respectively in the $\underset{\sim}{D}_M$ matrix.

APPENDIX D

The elements of $\underset{\sim}{D}$ matrix for the thick shell theory are defined here as follows. If we set

$$H_i = \frac{1}{i}(h^i_{L+1} - h^i_L)$$

$$H_i^- = (H_i - K \cdot H_{i+1})$$

$$H_i^+ = (H_i + K \cdot H_{i+1}), \quad \text{where } K = \frac{1}{R}$$

and i takes an integer value between 1 and 8, then the sub-matrix can be readily obtained in the following forms based on the geometrical assumption, $(h/R)^2 \ll 1$.

$$\underset{\sim}{D}_M = \sum_{L=1}^{NL} \begin{bmatrix} H_1^-Q_{11} & H_1Q_{12} & H_1^-Q_{13} & H_1Q_{13} & H_3^-Q_{11} & H_3Q_{12} & H_3^-Q_{13} & H_3Q_{13} \\ & H_1^+Q_{22} & H_1Q_{23} & H_1^+Q_{23} & H_3Q_{21} & H_3^+Q_{22} & H_3Q_{23} & H_3^+Q_{23} \\ & & H_1^-Q_{33} & H_1Q_{33} & H_3^-Q_{31} & H_3Q_{32} & H_3^-Q_{33} & H_3Q_{33} \\ & & & H_1^+Q_{33} & H_3Q_{31} & H_3^+Q_{32} & H_3Q_{33} & H_3^+Q_{33} \\ & & & & H_5^-Q_{11} & H_5Q_{12} & H_5^-Q_{13} & H_5Q_{13} \\ \text{Symmetric} & & & & & H_5^+Q_{22} & H_5Q_{23} & H_5^+Q_{23} \\ & & & & & & H_5^-Q_{33} & H_5Q_{33} \\ & & & & & & & H_5^+Q_{33} \end{bmatrix} L\text{th layer}$$

$$\underset{\sim}{D}_S = \sum_{L=1}^{NL} \begin{bmatrix} H_1^+Q_{44} & H_1Q_{45} & H_3^+Q_{44} & H_3Q_{45} & H_2^+Q_{44} & H_2Q_{45} & H_4Q_{45} \\ & H_1^-Q_{55} & H_3Q_{54} & H_3^-Q_{55} & H_2Q_{54} & H_2^-Q_{55} & H_4^-Q_{55} \\ & & H_5^+Q_{44} & H_5Q_{45} & H_4^+Q_{44} & H_4Q_{45} & H_6Q_{45} \\ & & & H_5^-Q_{55} & H_4Q_{54} & H_4^-Q_{55} & H_6^-Q_{55} \\ & & & & H_3^+Q_{44} & H_3Q_{45} & H_5Q_{45} \\ \text{Symmetric} & & & & & H_3^-Q_{55} & H_5^-Q_{55} \\ & & & & & & H_7^-Q_{55} \end{bmatrix} L\text{th layer}$$

The elements of the $\underset{\sim}{D}_C$ matrix are obtained by replacing H_1, H_1^+, H_1^-, H_3, H_3^+, H_3^-, H_5, H_5^+ and H_5^- by H_2, H_2^+, H_2^-, H_4, H_4^+, H_4^-, H_6, H_6^+ and H_6^- respectively in the $\underset{\sim}{D}_M$ matrix mentioned above. Similarly $\underset{\sim}{D}_B$ matrix is obtained by replacing H_1, H_1^+, H_1^-, H_3, H_3^+, H_3^-, H_5, H_5^+ and H_5^- by H_3, H_3^+, H_3^-, H_5, H_5^+, H_5^-, H_7, H_7^+ and H_7^- respectively in the $\underset{\sim}{D}_M$ matrix.